Available online at www.sciencedirect.com
ScienceDirect
Polymer 48 (2007) 574–578
polymer
www.elsevier.com/locate/polymer

High strain rate mechanical behavior of polyurea

C.M. Roland*, J.N. Twigg, Y. Vu, P.H. Mott

Chemistry Division, U.S. Naval Research Laboratory, Washington, DC 20375, United States

Received 5 October 2006; received in revised form 20 November 2006; accepted 27 November 2006
Available online 18 December 2006

Abstract

Stress–strain measurements are reported for an elastomeric polyurea in uniaxial tension over a range of strain rates from 0.06 to 573 s^{-1}. The experiments were carried out on a new drop weight test instrument, which provides mechanical data at strain rates up to 1000 s^{-1}, filling the gap between conventional low speed instruments and split Hopkinson bar tests. The tensile data obtained herein are compared with recent high strain rate compression data on the same material [Yi et al. Polymer 2006;47:319–29]. Advantages of the present measurements include a more uniform strain rate and the ability to ensure homogeneous strain.

Keywords: Polyurea; High strain rate; Viscoelasticity

1. Introduction

Elastomers are highly viscoelastic and thus their mechanical properties are strongly rate dependent. This property underlies many uses of rubber and is emphasized in applications involving high strain rates, such as the wet-skid resistance of tire treads [1–5], mechanical capacitors [6–8], and coatings for impact resistance [9,10] and acoustic damping [11–13]. Characterizing rubbery polymers at high strain rates is difficult, even at small amplitudes. Typical dynamic mechanical spectrometers are limited to frequencies below *ca.* 100 Hz, although custom-built instruments have attained $\sim 10^4$ Hz [14]. Atomic force microscopes (''nanoindenters'') operate as high as 1 MHz [15,16] but only probe the surface [17]. While time–temperature superpositioning is often invoked to extend the effective frequency range of test data, the results are inaccurate for measurements in the glass transition zone [18–22]. Unfortunately, this is the regime of interest if very high frequency results are required.

The difficulties of high strain rate testing are exacerbated if the behavior at high strains is to be measured. Even though unfilled rubber can be linearly viscoelastic to fairly large strains (*ca.* 100%) [23], it is generally not possible to apply Boltzmann superpositioning to deduce the properties at high strains from low strain experiments [24,25]. In recognition of this problem, much effort has been extended to develop methods that directly measure high strain, high strain rate properties [13]. The most common technique is the split Hopkinson bar (SHB) apparatus [26], which can measure at large strains (>300% in compression) and at very high rates (10^4 s^{-1}). Originally developed for metals, recently the SHB has been used to characterize the mechanical behavior of various elastomers [27–31]. Drawbacks of the test include the difficulty of ensuring homogeneous strain (barreling of the cylindrical test specimen introduces shear at the faces [32,33]) and a non-constant strain rate [26,28,31].

In this paper we report results obtained on a newly developed drop weight tensile test instrument [34]. Drop weight testers have a long history [35–38]. The present design was inspired by an apparatus of Hoo Fatt and coworkers [39,40], who modified a pendulum impact tester to obtain extensional stress–strain measurements at rates up to 480 s^{-1}. Our instrument is illustrated in Fig. 1. A 100 kg mass is dropped down a vertical track to engage L-levers, which displace shuttles to which the test specimen is attached. Equilibrium was ensured (and subsequently verified) by equal displacement of each end

* Corresponding author.
E-mail address: roland@nrl.navy.mil (C.M. Roland).

0032-3861/$ - see front matter © 2006 Elsevier Ltd. All rights reserved.
doi:10.1016/j.polymer.2006.11.051

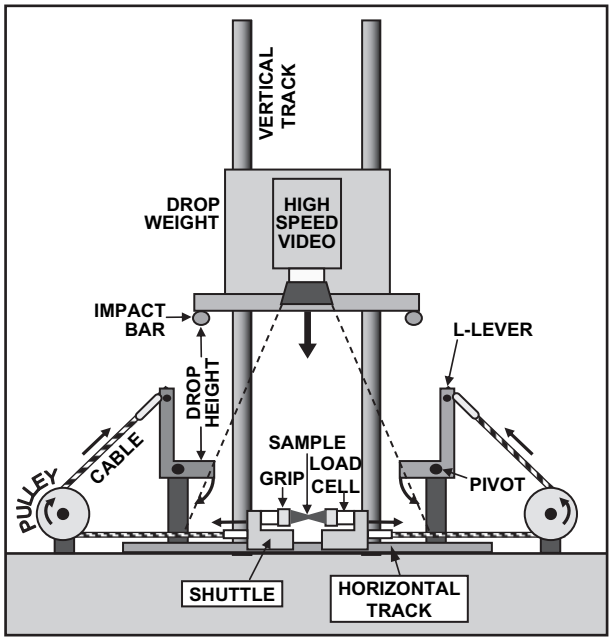

Fig. 1. Schematic of the high-speed tensile test instrument.

of the sample. Shuttle speeds as high as 26 m/s are achievable, corresponding to strain rates $\sim 10^3$ s^{-1}.

The material studied herein is an elastomeric polyurea. Polyureas are formed by the rapid reaction of isocyanates and amines. This fast reaction distinguishes them from polyurethanes – polyurea gel times are less than 1 min, which means that the reaction proceeds largely independently of ambient temperature and humidity, facilitating processing under diverse conditions. The extensive intermolecular hydrogen bonding of polyureas leads to ''tough'' mechanical properties. Polyureas have been used commercially for more than a decade. A recent application is as a protective coating on buildings, in order to minimize fragmentation of the structure (and consequent collateral damage to personnel) during a bomb explosion. Polyurea coatings have also been applied to military vehicles to mitigate damage from gunfire and explosives. Such applications, which involve impact loading, motivate the study of the mechanical response of the material under high strains and high strain rates.

2. Experimental

The polyurea was formed by the reaction of a modified diphenylmethane diisocyanate prepolymer (Isonate 143L from Dow Chemical; 144 g/eq) with an oligomeric diamine curative (Versalink P1000 from Air Products; 600 g/eq). Except where noted, a ratio of 1:4 prepolymer to curative by weight was used herein (96% stoichiometry, as recommended by the manufacturer [41]). The polyurea was processed with an internal mixer, and sprayed into sheets for curing at room temperature. After annealing at RT for at least 1 month, test specimens (ASTM D4482) were die cut from the cast sheets.

For the high-speed testing, strains were determined from the position of fiducial marks, using a digital camera (Vision Research Phantom 7 monochrome). Images (704 × 96 pixels) were recorded in 12-bit resolution at 10^4 frames/s. The video was analyzed using commercial software (Image Express Motion Plus) to obtain the position of the marks as a function of time during a test. Stresses were measured with two load cells (Fig. 1): conventionally by a strain-gauge type (Futek LCM300) and for fast measurements with a piezoelectric load cell (PCB Piezotronics, Inc. Link ICP Quartz Force Sensor), which self-discharges in a few seconds. To measure and correct for inertia, accelerometers (PCB Piezotronics, Inc. Quartz Shear ICP Accelerometer) were attached to the shuttles. Additional measurements were made at low strain rate <0.1 s^{-1} using an Instron 5500R with strains determined by an optical extensometer.

3. Results

3.1. Influence of stoichiometry on low strain rate response

The stress–strain curve measured at 0.06 s^{-1} strain rate is shown in Fig. 2. The material initially exhibits a high modulus, defined as the slope of the engineering stress *vs.* strain curve (strain, ε, defined as the change in length over the initial length) = 27 MPa. Following this initial linear region the material yields at $\varepsilon \sim 70\%$ elongation, with a subsequent slow rise in stress to failure at 620% elongation. These are very good mechanical properties, *i.e.*, high stiffness and elongation, associated with a tough elastomer. Interestingly, when the chemistry of the polyurea is altered by 5–10%, there is an enormous change in the mechanical properties. The yield stress varies inversely with stoichiometry, while the failure strain increases with increasing curative. These results show that increasing the amount of diisocyanate is necessary to drive the crosslinking reaction toward completion. The toughness, defined as the strain energy to failure, is shown in the inset of Fig. 2 as a function of the stoichiometry. Interestingly, despite the differences in the mechanical behavior, the toughness is

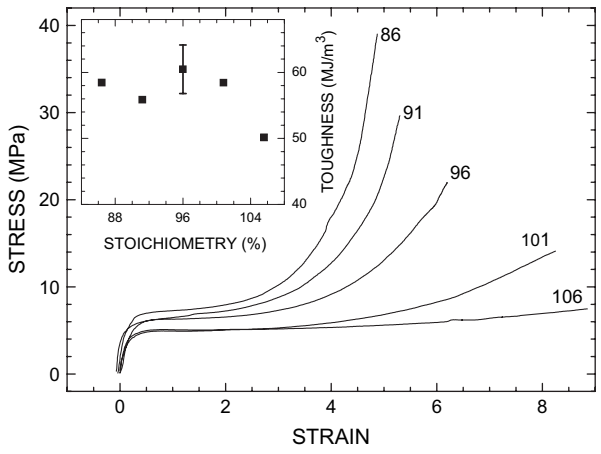

Fig. 2. Stress–strain curves obtained using an Instron for polyureas prepared with the indicated % stoichiometry. The strain rate for all tests was 0.06 s^{-1}. The inset shows the toughness (integral of stress–strain curve); error bars are one standard deviation.

essentially constant; that is, decreasing elongation to failure is compensated by the increase in stiffness of the material. Generally the effect of stoichiometry on the mechanical response of polyureas and polyurethanes is a complex interplay of crosslinking, hydrogen-bond formation, and degree of phase separation of the hard and soft domains [42–45].

Samples with a 96% stoichiometric ratio, used in the high-speed testing, fell in the mid-range of the data in Fig. 2. The sensitivity to small variations in the relative concentration of the components introduces some uncertainty into comparisons made to results from other laboratories (see below).

3.2. Inertial effects at high speeds

Usually inertial forces are negligible in conventional mechanical measurements because accelerations are only on the order of 0.01 m/s^2. This is not true for the high rate experiments herein, in which respective shuttle speeds and accelerations as high as 10 m/s and 2000 m/s^2 were attained. This is illustrated in Fig. 3, showing the force as a function of time measured with the two load cells. These data include the force necessary to accelerate the grips and other hardware. The inertia was quantified by tests *sans* specimen, with both forces and shuttle accelerations measured separately. The obtained inertial masses (conventional load cell, 12 g; piezoelectric load cell, 41 g) agreed with the respective weights of the hardware. The inertial forces in Fig. 3 were found from the product of the inertial mass and the measured acceleration, the latter determined from the accelerometers and equal to the (much noisier) second derivative of the displacement *vs*. time data extracted from the video images. The two curves have similar shapes, but with different amplitudes due to the different masses of the respective load cells. Correcting for inertia changes the shape of the stress–strain curves significantly, with the two load cells now yielding equivalent results (Fig. 3).

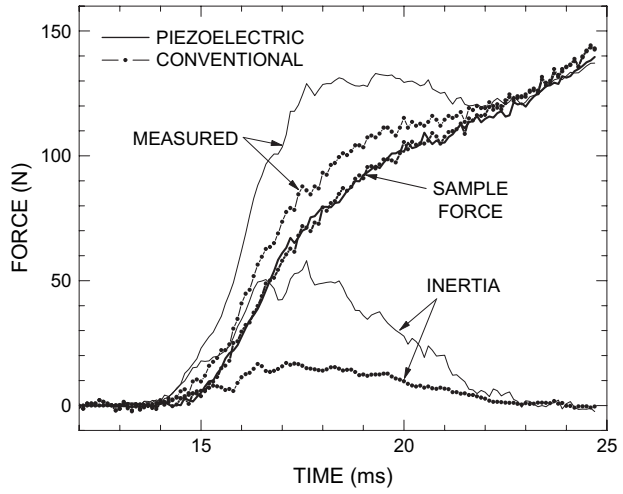

Fig. 3. Effect of inertia on load-deflection curve for a 0.6 m drop height (maximum shuttle speed = 9.7 m/s). The data from the two transducers differ due to their different masses and hence different inertial contributions to the measured force. Subtraction of the inertial force yields equivalent loading curves.

3.3. High strain rate results

Fig. 4 displays the engineering stress–strain curves measured at three drop heights (strain rates = 327–573 s^{-1}), along with the results using a winch motor to lower the weight (rate = 14 s^{-1}) and from an Instron test (rate = 0.15 s^{-1}). The initial region is linear, with a modulus (slope) approaching 100 MPa at the highest rate. Although the yield strains are comparable, the yield stress increases by more than a factor of 2 over this range of rates. As expected from general viscoelastic behavior, the failure stress increases and the failure strain decreases with strain rate, although repeat testing would be required to obtain statistically significant failure properties.

In Fig. 5 we plot the true (Cauchy) stress σ_T ($=\sigma/(\varepsilon+1)$) as a function of true (Hencky) strain, ε_T ($=\ln(\varepsilon+1)$), and include

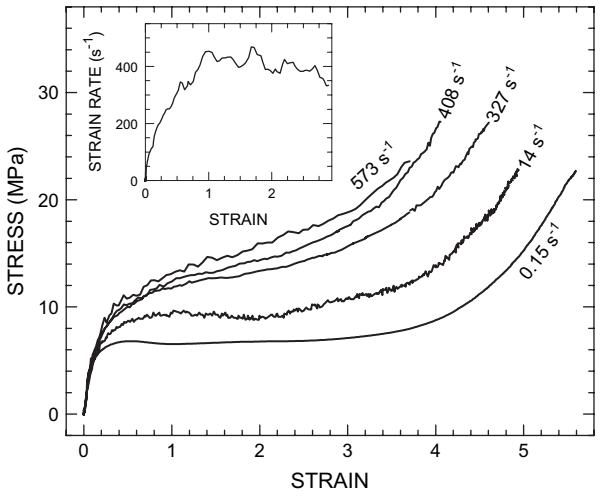

Fig. 4. Engineering stress *vs*. strain measured on an Instron (lowest curve), using a winch to lower the drop weight (second curve from bottom), and for drop heights equal to 0.152, 0.305, and 0.61 m (middle through uppermost curves, respectively, all corrected for inertial forces), with the corresponding engineering strain rates as indicated. The inset shows the typical variation of strain rate over the course of a test.

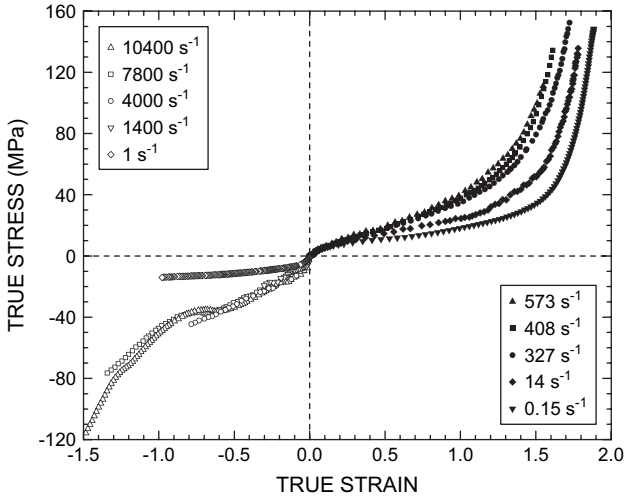

Fig. 5. Data in Fig. 4 (solid symbols) plotted as true stress *vs*. true strain, along with SHB compression results and one slow strain rate curve from Ref. [31] (hollow symbols). SHB strain rates are averages.

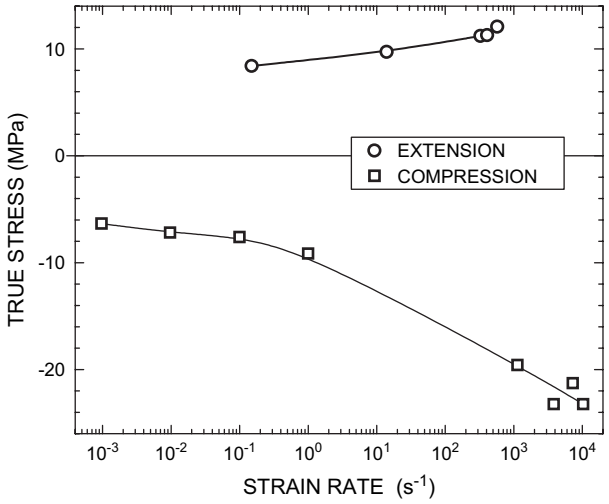

Fig. 6. True stress at $\varepsilon = 0.3$ as a function of strain rate for extension (circles) and compression (squares), the latter from Ref. [31].

SHB compression results on the same polyurea, as well as one low strain rate measurement from an Instron [31]. Near the origin ($|\varepsilon_T| < 1/2$) the tension data have a lower slope, consistent with the behavior expected for elastic equilibrium – the modulus is a decreasing function of tensile strain due to mitigation of the entanglement constraints [46]. However, in compression this effect is weaker or absent [47,48].

The other noticeable difference between the two sets of data in Fig. 5 is the apparent effect of strain rate. While for tension there is an expected continuous increase in stiffness with increasing rate, the compression data become essentially invariant to rate at the high strain rates. In Fig. 6 the true stress for $\varepsilon = 0.3$ is plotted *vs.* the (engineering) strain rate, with the inclusion of low rate (Instron) compression results [31]. The modulus in compression varies monotonically with rate for low strain rates, with a marked change on going from 1 to 1000 s^{-1}; the change in the rate dependence over this range is much larger than for tension. These results, however, must be interpreted with some caution, given the sensitivity of the mechanical properties to stoichiometry (Fig. 2). Also it should be noted that the strain rate in an SHB experiment increases with strain [31], so that the values for compression in Fig. 6 are averages.

We also note that there does not appear to be any indication of a transition from rubbery to glassy behavior in the results of Fig. 6, as had been suggested by Yi et al. [31]. Dielectric relaxation measurements on this material indicate a broad glass transition zone centered at 10^6 Hz at room temperature [49].

4. Summary

Stress–strain measurements were carried out on a polyurea using a newly developed drop weight tester, capable of achieving large tensile strains at high strain rates. The results presented herein demonstrate that material properties can be obtained, free of artifacts due to inertia, inhomogeneous strains, and non-constant strain rates. Data from this instrument fill a gap between conventional, low-rate stress–strain curves and SHB measurements.

Acknowledgements

We thank H.S. Schrader for experimental assistance and D.P. Owen for preparing the polyurea. This work was supported by the Office of Naval Research. Y. Vu is grateful for a National Research Council postdoctoral fellowship.

References

[1] Heinrich G. Rubber Chem Technol 1997;70:1.
[2] Kluppel M, Heinrich G. Rubber Chem Technol 2000;73:578.
[3] Persson BNJ, Tartaglino U, Albohr O, Tosatti E. Phys Rev B 2005;71:035428.
[4] Bond R, Morton GF, Krol LH. Polymer 1984;25:132.
[5] Rahalkar RR. Rubber Chem Technol 1989;62:246.
[6] Hoppie LO. Rubber Chem Technol 1982;55:219.
[7] Choi IS, Roland CM, Bissonnette LC. Rubber Chem Technol 1994;67:892.
[8] Little J. Undersea Warfare 1999;1:12.
[9] Davidson JS, Porter JR, Dinan RJ, Hammons MI, Connell JD. J Perform Constr Facil 2004;18:100.
[10] Roland CM. Rubber technologist's handbook, vol. 2. Shrewsbury, UK: RAPRA, in press.
[11] Sound and vibration damping with polymers. In: Corsaro RD, Sperling LH, editors. ACS symposium series 424. Washington, DC: American Chemical Society; 1990.
[12] Mott PH, Roland CM, Corsaro RD. J Acoust Soc Am 2002;111:1782.
[13] Roland CM. Rubber Chem Technol 2006;79.
[14] Fitzgerald ER, Fitzgerald RE. Polym Bull 1987;18:167.
[15] Van Landingham MR, McKnight SH, Palmese GR, Eduljee RF, Gillespie JW, McCullough RL. J Mater Sci Lett 1997;16:117.
[16] Dupas E, Gremaud G, Kulik A, Loubet J-L. Rev Sci Instrum 2001;72:3891.
[17] Mareanukroh M, Eby RK, Scavuzzo RJ, Hamed GR. Rubber Chem Technol 2000;73:912.
[18] Ngai KL, Plazek DJ. Rubber Chem Technol 1995;68:376.
[19] Plazek DJ. Polym J 1980;12:43.
[20] Plazek DJ, Chay I-C, Ngai KL, Roland CM. Macromolecules 1995;28:6432.
[21] Roland CM, Ngai KL, Santangelo PG, Qiu XH, Ediger MD, Plazek DJ. Macromolecules 2001;34:6159.
[22] Santangelo PG, Roland CM. Macromolecules 1998;31:3715.
[23] Yannas IV. J Polym Sci Macro 1974;9:163.
[24] Roland CM. Rubber Chem Technol 1989;62:880.
[25] Santangelo PG, Roland CM. Rubber Chem Technol 1992;65:965.
[26] Nemat-Nasser S, Isaacs JB, Starrett JE. Proc R Soc London Ser A Math Phys Sci 1991;435:371.
[27] Sharma A, Shukla A, Prosser RA. J Mater Sci 2002;37:1005.
[28] Song B, Chen W. Trans ASME 2003;125:294.
[29] Shim VPW, Yang LM, Lim CT, Law PH. J Appl Polym Sci 2004;92:523.
[30] Quintavalla SJ, Johnson SH. Rubber Chem Technol 2004;77:972.
[31] Yi J, Boyce MC, Lee GF, Balizer E. Polymer 2006;47:319.
[32] Mott PH, Roland CM. Rubber Chem Technol 1995;68:739.
[33] Yeoh OH, Pinter GA, Banks HT. Rubber Chem Technol 2002;75:549.
[34] Mott PH, Twigg JN, Roland DF, Schrader HS, Roland CM. Rev Sci Instrum, submitted for publication.
[35] Albertoni GJ. Rubber Chem Technol 1937;10:317.
[36] Roth FL, Holt WL. Rubber Chem Technol 1940;13:348.
[37] Villars DS. J Appl Phys 1950;521:565.
[38] Gale A, Mills NJ. Plast Rubber Process Appl 1985;5:101.
[39] Hoo Fatt MS, Bekar I. J Mater Sci 2004;39:6885.
[40] Bekar I, Hoo Fatt MS, Padovan J. Tire Sci Technol 2002;30:45.

[41] <www.airproducts.com/NR/rdonlyres/6DCACE34–0B21-4ED5-B3B9-A9B102713874/0/14005050US.pdf>.
[42] Urbaczewski-Espuche E, Galy J, Gerard JF, Pascault JP, Sautereau H. Polym Eng Sci 1991;31:1572.
[43] Shenoy MA, D'Melo DJ. Surf Coat Int Part B Coat Trans 2006;89221.
[44] Stanford JL, Still RH, Wilkinson AN. Polymer 1995;36:3555.
[45] Li ZF, Xu CM, Yin SM, Wen LR. Spectrosc Spectral Anal 2002;22:774.
[46] Erman B, Mark JE. Structure and properties of rubberlike networks. New York: Oxford University Press; 1997.
[47] Roland CM, Mott PH. Macromolecules 1998;31:4033.
[48] Mott PH, Roland CM. Macromolecules 1996;29:6941.
[49] Bogoslovov R, Roland CM, to be published.